84. Spectra of Organic Molecules in Thin Films

by **J.D. Swalen, M. Tacke**[1]**, R. Santo, K.E. Rieckhoff**[2] and **J. Fischer**[3]

IBM Research Laboratory, San José, California 95193

In Memorial to Professor *Heinrich Labhart*

(11.XI.77)

Summary

In order to investigate molecules and their interactions at interfaces we have developed a new spectroscopic technique based on integrated optics. A significant increase in sensitivity has been predicted and observed. We report here the details of the method and some preliminary spectra of organic dye molecules on thin films.

During the academic year 1972–73 in the laboratories of Professor *Labhart*, one of the authors (*J.D.S.*) had the opportunity to initiate work on the spectroscopic study of molecules on the surfaces of thin films. Molecules on surfaces and in thin films can behave structurally and chemically differently from molecules in the bulk or gas phases and it was our intent to develop a sensitive spectroscopic technique to observe these changes. Besides the investigation of structural modifications at an interface and reactivity at an interface, it was also our desire to construct sandwich structures of molecules between metal electrodes for electrochromic measurements, a long standing interest of Professor *Labhart* [1] [2]. To us the new approaches of integrated optics seemed to be a very sensitive and convenient way to perform an ATR (attenuated total reflection) type experiment on the thin films. A clean separation of polarization was possible, making possible the observation of the extraordinary light ray not mixed with the ordinary ray: the usual case with oblique propagation through a film [2] [3]. In addition, high optical fields are present in the wave guides varying across the guides in patterns with nodes and antinodes, the location and number depending on mode number. Hence both the orientation or orientational distribution and location in the film of the molecules interacting with the radiation can be derived from a detailed analysis of the mode structure. In the development of this technique and its application to spectroscopy, a number of ancillary tasks were first required, such as film fabrication, molecular deposition, laser spectroscopic apparatus, integrated optical parts and rotating table and computer programs for the analysis of the data and interpretation of the observed

[1]) Present address: Physik. Inst. der Universität, Würzburg, Germany.
[2]) Present address: Physics Dept., *Simon Fraser* University, Burnaby, B.C. Canada.
[3]) Present address: *Ciba-Geigy AG*, Basel, Switzerland.

phenomena and effects. It is the purpose of this paper to describe the experimental approach and present some of the data obtained on dye molecules in and on films. Since various parts have been already published [4–6], these results will be only described briefly to give a total picture. More details can be obtained in these works.

Three related methods for the optical study of thin films, and particularly molecules on or in the films, are ATR, ellipsometry and surface plasmon resonance. In the ATR technique, usually applied in the infrared, the light reflects back and forth in a thin plate of germanium, or other material, interacting with the molecules adsorbed on the surface [7]. Essentially this is the same procedure as the wave guide approach except in the latter many more reflections occur, approximately 30 to 40 times, and the possibility exists of placing molecules internal to the film in higher optical fields. Sensitivity, therefore, with integrated optics can be intrinsically much higher.

Ellipsometry is reflection, normally done at a fixed angle and at a fixed wavelength. Both intensity and phase are recorded from which film thickness and refractive index can be derived [8] [9]. With absorbing molecules, measured as a function of wavelength, ellipsometry can be a very sensitive and effective method for the study of surface molecules [10]. Fixed angular measurements also have the advantage for vacuum systems of fixed angles to windows, thus avoiding the problem of reflectivity changes during the experiment.

Surface plasmons [11] on metal surfaces where the optical field is concentrated at the interface between the metal and air, is sensitive to overcoatings of dielectrics. Studies have been done of silver films covered by thin layers of LiF [12] [13], pump oil [14], silver sulfide tarnish [12] [15], amorphous carbon [12] [13], and monolayers of cadmium arachidate [17] (also on gold films [18]). Infrared studies of benzoic acid and rhodamine 6G [19] and manganese arachidate [20] have also been reported. *Abelès et al.* [15] [16] used ellipsometric techniques for the measurement of surface plasmon resonances, while all the others employed the standard prism coupling technique [21]. With these resonances both the real and imaginary parts of the dielectric function of a thin monolayer film can be derived from the reflectivity as a function of wavelength.

In comparing the wave guide approach to these three discussed methods, it appears to be a more sensitive technique for measurements at dielectric-dielectric interfaces but has some limitations. These points will be discussed as we describe the method. Mathematical details on analyses of optical wave guides have been placed in the Appendix.

Film preparation. The preparation of uniform, optically good films is not easy and required the development of good procedures and techniques [6]. For polymeric films to overcoat molecular layers, it was most convenient to use a water soluble polymer so as not to disturb the layers and their optical quality. Poly(vinyl alcohol) (PVA) and poly(vinly pyrrolidone) (PVP) were two polymers that made good films rather readily, but care had to be taken to anneal and bake the films at 60° to remove the water. Most commonly, we used the doctor blading technique for making the films. This consists of pushing a solution by a blade some 0.05 to 0.1 mm over the substrate. Uniform velocity and constant blade spacing (wet gap) require some motor driven equipment and accurate mechanical spacing controls. We used a stepping motor to move the substrate pass the blade which was set with micrometer screws. Other techniques are spinning, dipping and horizontal flow; each of these is described in [6].

Concerning the substrates themselves, they must be carefully cleaned, of optical quality, *i.e.*, pitch polished smooth and flat but only to a wavelength, and of low refractive index to be totally internally reflecting for most polymeric thin films. To satisfy these conditions we selected fused silica, 3 mm thick for strength. Pyrex could also have been used, except that its refractive is slightly higher than that of fused silica. One further advantage of fused silica is that its refractive index is rather completely tabulated in [22]. A least squares fit of the power series dispersion equation, like that due to *Cauchy* [23], to all the data gives the refractive index (accurate to ± 0.00001) of fused silica as a function of wavelength over the visible spectral region:

$$n = 0.004997\lambda^{-2} - 0.010433\lambda^{-1} + 1.473387 - 0.023189\lambda + 0.005915\lambda^2$$

where λ is the wavelength in microns.

Another approach, which we have found to be very useful because of the higher internal optical fields, was that in which the molecules were sandwiched between two conducting layers of optical wave guide [24]. Sputtered glass films of *Corning* 7059 glass were deposited on our quartz substrates by our thin film service group. The molecules were then deposited and overcoated with PVA or PVP. [5] and [6] give some of the theoretical analysis of this structure which can be combined with the results given in the Appendix.

The molecular films which were investigated, were deposited by either the *Langmuir-Blodgett* technique [3] shown schematically in *Figure 1* or by vacuum evaporation. Generally with the sensitivity

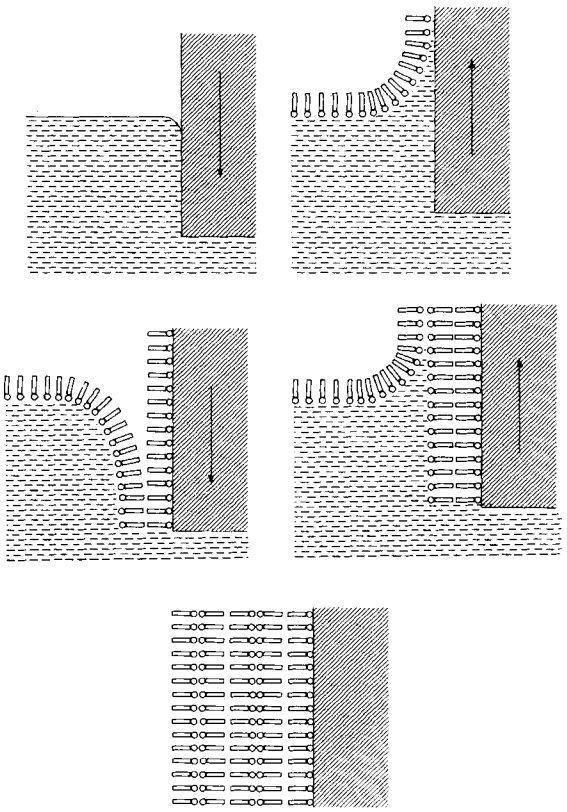

Fig. 1. *Schematically the monolayer deposition procedure is illustrated for a hydrophilic surface.* First the substrate slide is lowered into the *Langmuir Blodgett* trough. On spreading from a solution the monolayer onto the water surface and compressing it with a float, the substrate is slowly drawn out of the water and a monolayer transferred. Subsequent dippings transfer two layers first to the hydrophobically created surface on the down motion and then to the hydrophilically created surface on the up motion. The completed structure for Y deposition is a head to head, tail to tail arrangement.

of the method, a few non absorbing monolayers, in which only a few molecules were embedded depending on their oscillator strength of the transition studies, were sufficient. Two configurations were used: one with complete coverage of the slide and the other with half coverage down the length of the slide. Because scattering losses contribute to the signal attenuation, much like absorption, the split film gave a comparison between conduction of light with only scattering losses and conduction attenuated by both scattering and absorption. These points will be discussed more below in our discussion of integrated optics and spectroscopy.

Integrated optics. Integrated optics [25-28] is the conduction of light through a thin film of the order of a few microns thick in a wave guide type mode. By a ray optics approach the light can be considered to be reflected back and forth between the two interfaces, usually air and the substrate. At each interface, *i.e.*, air-film and film-substrate, the light undergoes total internal reflection because both surrounding materials have lower refractive indices than the film. For a mode structure and propagation the phase shifts at each reflection plus that due to the phase shift in transmission through the film must add to a multiple of 2π. In the course of light conduction for one centimeter some 600 reflections usually will take place, giving a large enhancement for an ATR experiment. As mentioned even larger improvements in the signal to noise ratio are possible by having the molecules under investigation between two guiding films [4] [24]. In *Figure 2* the optical electric field intensity is plotted for three TE modes in an optical wave guide of 2 micron thickness. Notice that the modes are numbered by the number of nodes. Molecules embedded in the film will interact with different modes differently because the intensity varies with the depth within the film. Molecules on the surface see higher fields from the higher order modes. *Figure 2* was made from a calculation using *Maxwell*'s equations and matching the boundary conditions at each interface. In the Appendix we derive the eigenvalue equations, the internal fields, and the improvement in sensitivity of wave guide spectroscopy over conventional oblique irradiation of a film [3]. The related *Fresnel* reflection equations, and our method of computer programming for their solution are also covered. With absorption, we have a much more complicated situation than that which occurs in light conduction through dielectric films with no loss [25-28]. Many of the variables become complex. In our case we either solved the eigenvalue equation by perturbation calculations for small absorption or solved the reflectivity by the *Fresnel* equations in complex form, much as we have done in the plasmon work [17] [18].

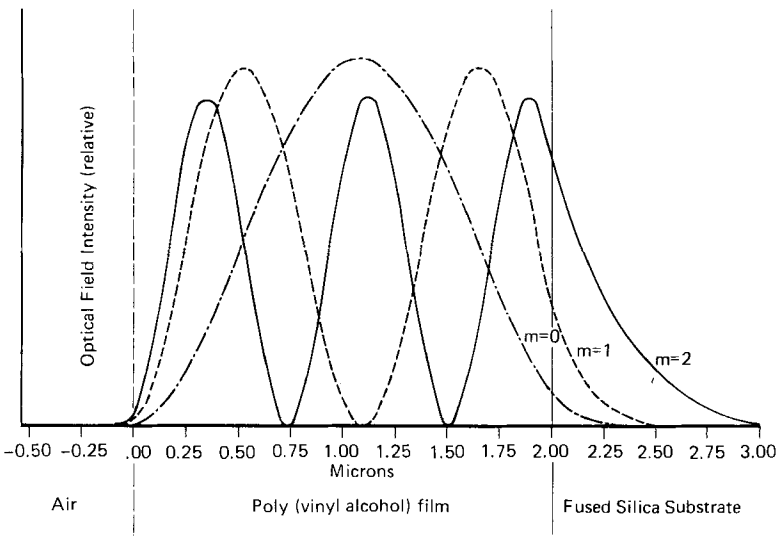

Fig. 2. *The square of optical electric field across an optical wave guide.* The number of modes are designed by the m values of the guided wave. Notice that the evanescent field extends more into the substrate, with a refractive index closer to that of the film, than into air. Also the higher m modes have larger evanescent tails.

Experimentally we excited conduction in the guides by prism coupling [27] [28], shown schematically in *Figure 3* where the laser beam is totally internally reflected from the bottom of the prism which is made of a high index glass (*Schott* LaSF5) to allow a large range of propagation vectors for coupling. Coupling is accomplished by pressing the prism close to the film, usually with some clamping arrangement, so that the evanescent wave feeds the guide. *Figure 4* is an experimental tracing from our recorder showing the modes as a function of angle ϕ of *Figure 3*. Weak coupling is evidenced by the facts that the first modes are weaker and all modes have about the same half-width. Overcoupling leads to errors from both angular shifts and mode half-widths. A theoretical plot with three different gap widths shows in *Figure 5* a shift to larger angles with increased coupling at smaller gaps. We always attempted to achieve the minimum coupling without the loss of too much signal.

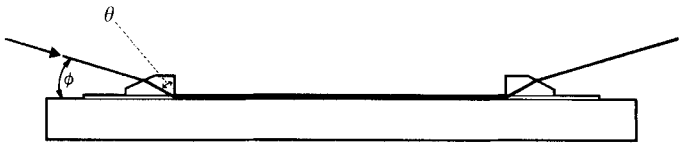

Fig. 3. *A schematic showing the prism couplers into and out of the thin film, shown enlarged on the surface.* The external angle ϕ is changed by rotating the substrate on a rotating table. The related internal angle θ changes the propagation constants k_z to match each mode.

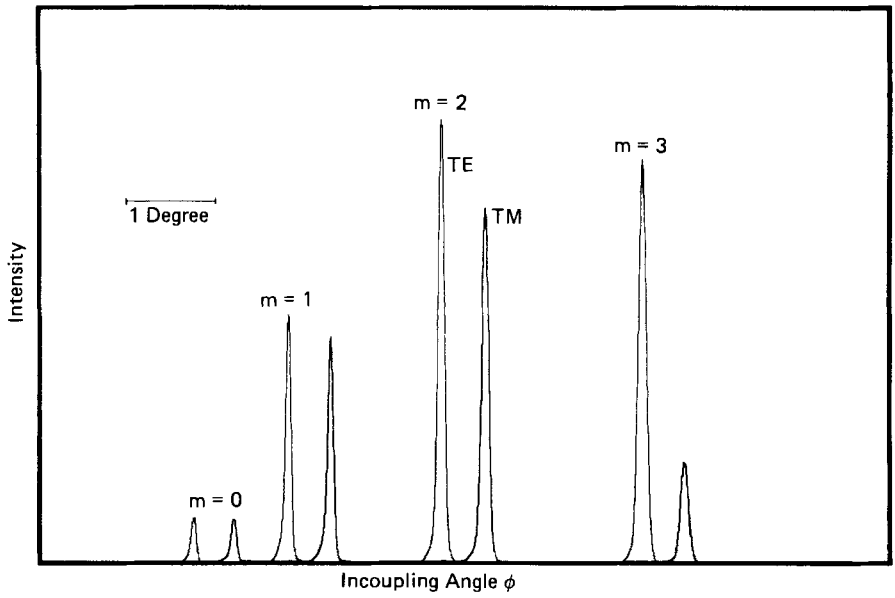

Fig. 4. *Recorded modes, intensity of outcoupled laser light,* versus *external angle.* Weak coupling is evidenced by the lower signal strength of the low order modes.

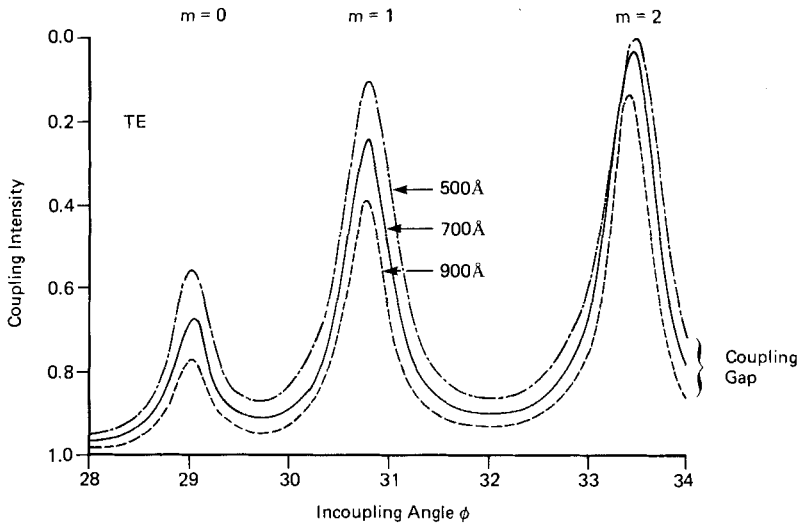

Fig. 5. *Theoretical calculations with the* Fresnel *coefficients for reflectivity at couplings of 500Å, 700Å and 900Å.* Small shifts in angle can be seen, resulting in errors if corrections are not made. Weak coupling, as shown in Fig. 4, is recommended.

Spectroscopic methods. Our first loss measurements were done on neat polymeric films [6] where we used the drop in intensity of scattered light along the track [29–31]. In order to separate absorption from scattering from inhomogenities along the film and in order to determine I_0 accurately, more complicated optical arrangements were tried and are schematically illustrated in *Figure 6*. The first arrangement is for direct absorption. By positioning or moving the outcoupling prism along the track a measure of the combined absorption and scattering losses can be obtained but we do not have a measure of I_0. The second arrangement uses two closely spaced prisms to obtain I_0 and to balance coupling intensity across the film. The long track through the gap between the two prisms gives I_{abs} at the distant prism.

In arrangement 3 we vibrated the beam with a vibrating mirror from a region with no absorbing molecules to one with them. A phase sensitive detector was tuned to this frequency and measured $I_0 - I_{abs}$. A second phase sensitive detector, which was tuned to the frequency of a chopper, measured $I_0 + I_{abs}$. From these two measurements, both I_0 and I_{abs} could be determined. Because the mode pattern shifts with absorption or the fact that the film may be not uniform, the spectra were measured at an angle at which the coupling efficiency was the same for both beams. This was accomplished by matching the intensities of the back reflected beams from the polished back face of the incoupling prism. *Figures 7* and *8* show two spectra taken by this method. The laser wavelength was changed point by point either from one laser to another, or to another lasing transition, or by tuning a dye laser. These spectra show from the TE/TM dependency that some molecules are oriented in the plane of the film and others perpendicularly. In particular the stilbene IV is clearly

seen in *Figure 7* to be oriented perpendicularly to the plane of the film – an unusual orientation for an evaporated dye. Interestingly the related azo molecules orient in the plane of the film. Further a hydrophilic substrate is needed for this orientation which optimized the electrochromic measurements [2] because the transition moment and the externally applied field could be aligned parallel or antiparallel. For the cyanine dye (II) the molecular structure and the film structure (see *Figure 1*) lead one to expect the opposite orientation to that of the stilbene and in fact this is born out in the spectrum shown in *Figure 8*. Our ratio of dimer to monomer, however, is somewhat smaller than that reported [3] and must represent some subtile differences in film growth and preparation.

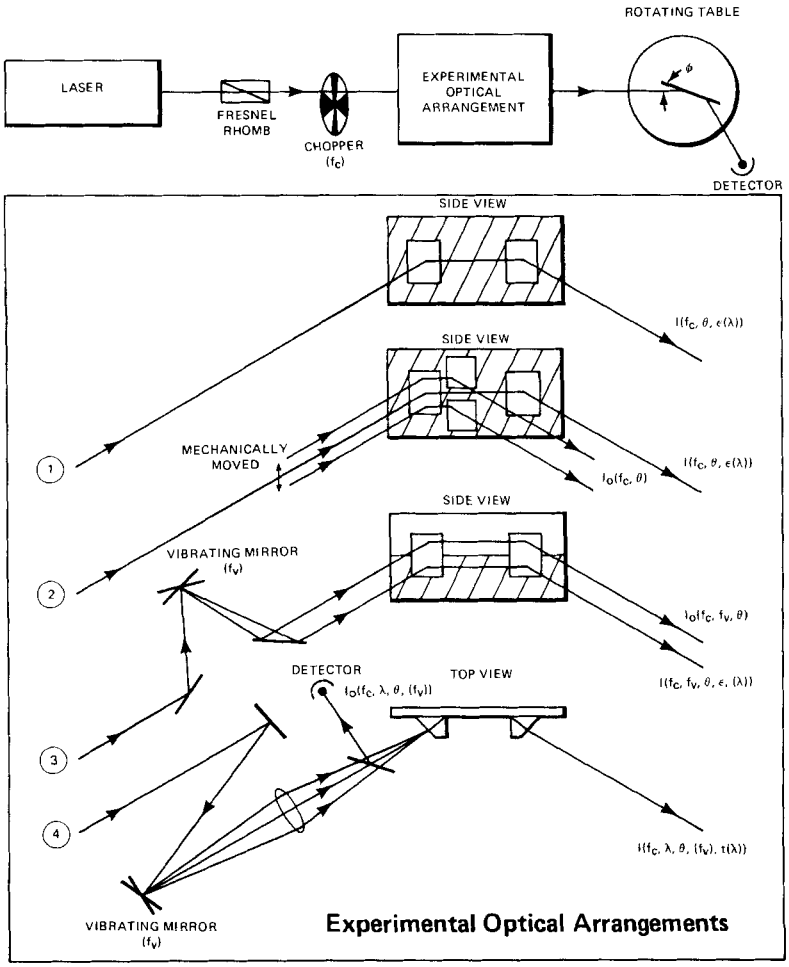

Fig. 6. *Experimental arrangement for optical spectroscopy by integrated optics.* For all experiments a laser source, polarizer and chopper were used as well as a rotating table with a goniometer arrangement so that the detector followed at 2ϕ. The four optical schemes show direct absorption, balanced absorption, double beam absorption by a vibrating mirror and a vibrating angular scan to scan over a whole mode allowing an additional wavelength scan.

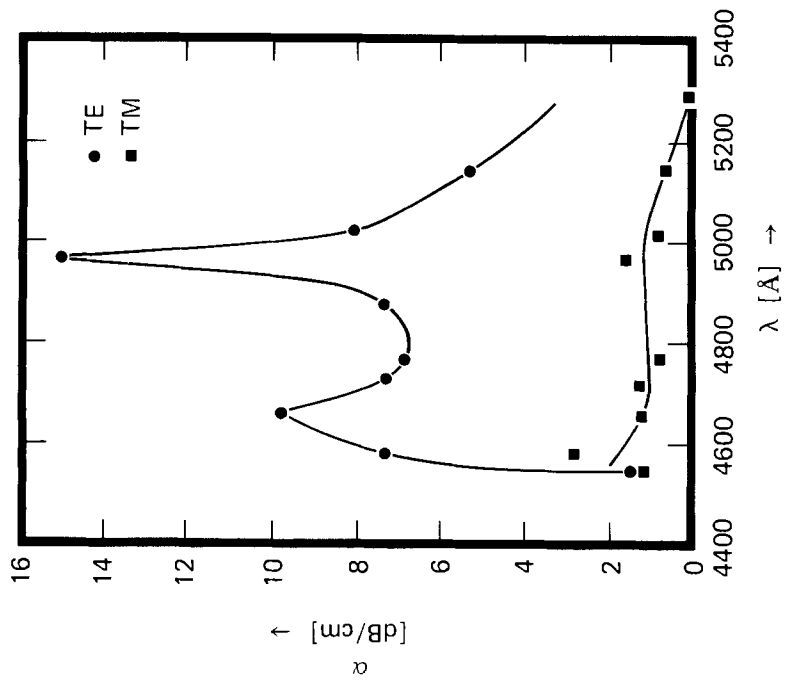

Fig. 8. *Additional absorption in the m = 1 mode of an optical wave guide of fused silica substrate from seven monolayers of cyanine dye* (compound II in *Fig. 9*) *in a 1:20 ratio of cadmium arachidate.* The molecular film is located between the film and substrate.

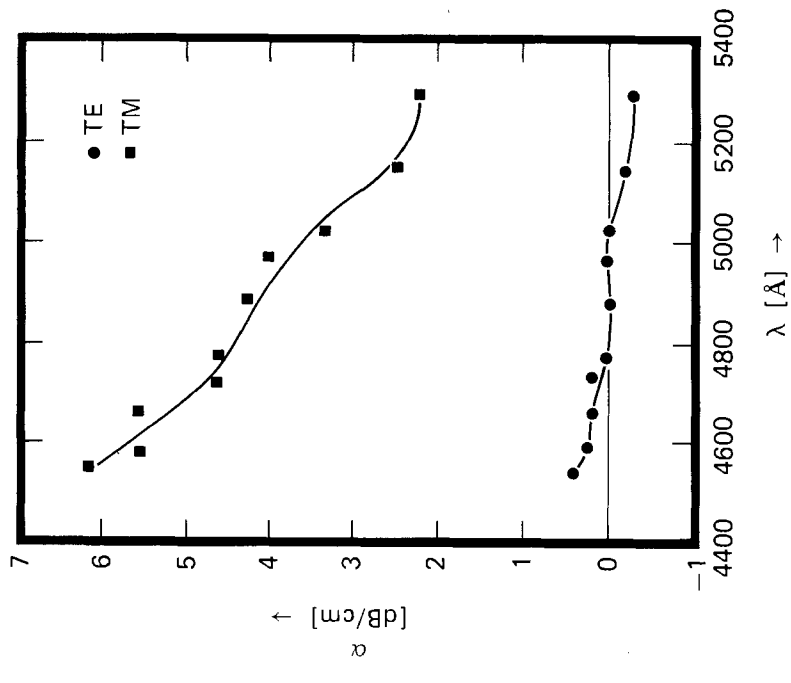

Fig. 7. *Additional absorption in the m = 1 mode of an optical wave guide of PVA on a fused silica substrate from a thin evaporated layer of 4-dimethylamino-4'-nitrostilbene* (compound IV in *Fig. 9*) *between the film and substrate.* The ordinate scale is 10× O.D./cm and can be converted to absorption coefficient by dividing by 4.343 (10 log e).

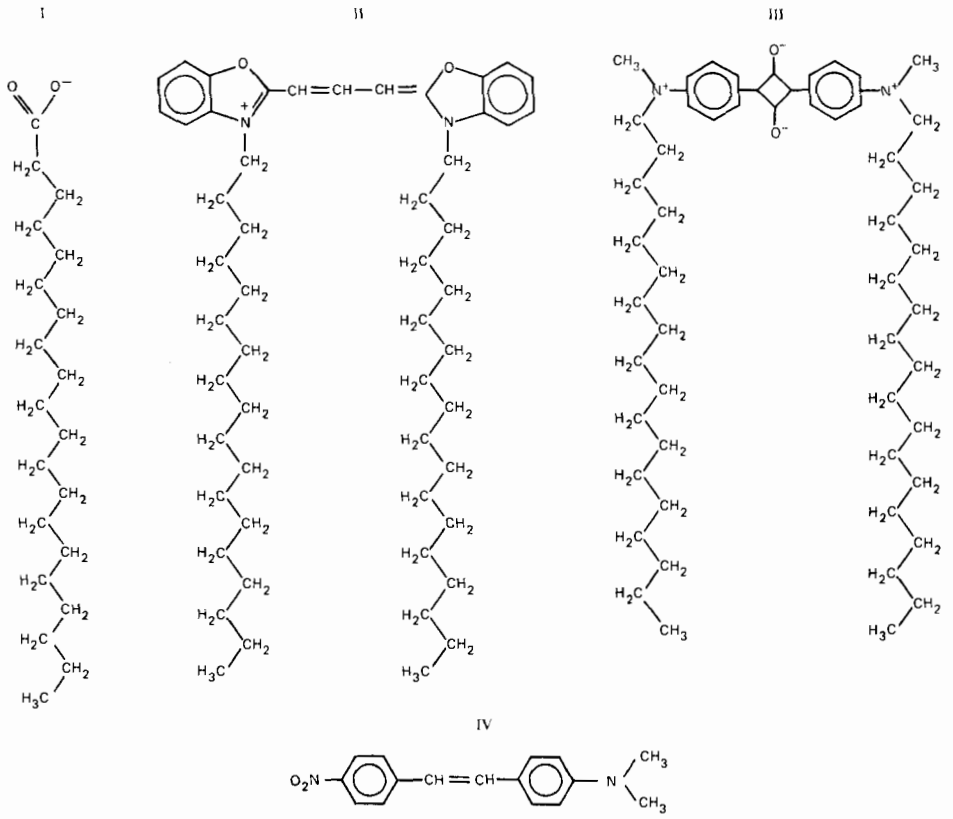

Fig. 9. *Molecular geometry of molecules studied. (I) arachidate ion, (II)* N,N′*-dioctadecyl-oxacarbocyanine, (III) squarylium, (IV) 4-dimethylamino-4′-nitrostilbene.*

Squarylium (III) exhibits a similar orientation to that of cyanine, as expected from its related molecular structure of two tails and a π appearance. The spectrum from the long axis transition is shifted, however, to the red.

The last experimental arrangement, which we will discuss – clearly many other variations on a theme exist – scans angle by a vibrating mirror (note, the different plane of vibration from that of arrangement 3) through a lens. I_0 was determined by a back reflection. With this arrangement a complete mode can be scanned during a sweep cycle. Provided the mode does not move off, wavelength can also be scanned to facilitate a more rapid recording of a spectrum. Vibrating the angle was usually done at twice the frequency of the chopper, giving both a forward and reverse trace during one period. In general we found we could scan some 500 to 600 Å by this procedure.

Conclusions. Although we have found integrated optics to be a very sensitive method for the spectral measurement of molecules on optically clear dielectric surfaces, the determination of I_0 is not easy, especially with variations incoupling

strength and film uniformity. Optically good films are needed which exhibit low scattering losses. Fortunately many of the polymeric films, we have made, were very good in this respect [6]. Also sputtered glass films can have very good optical quality with few scattering cracks. Repeated use is also possible, much like the plates in conventional ATR spectroscopy, except care must be taken in their cleaning. The advantage of re-use is that the optical constants of the film would be well characterized. One does lose a little sensitivity, however, placing the molecular films on the air side as opposed to the substrate side (see *Fig. 2*). Finally, much of our work has been point by point spectroscopy, much like the 1920's and 1930's, and as such was tedious.

As our work on surface plasmon [17] and on XPS [32] has shown molecules directly at an interface exhibit different bonding and structural characteristics. It is our intent to investigate more thoroughly with this thin film spectroscopy molecular interactions at interfaces. The high sensitivity to changes in both the real and imaginary parts of the dielectric function make these investigations feasible. Hence we consider that the methods described in this paper, when combined with other surface characterization techniques, can give us new insights to molecular interactions at an interface from orientational and energy shifts for the molecules.

For encouragement and support and the scientific discussions with the late Professor *Heinrich Labhart* which made the initiation of this work possible, we are very grateful. Much help from his secretary *H. Böckli* was also greatly appreciated. The monolayer techniques were learned in the laboratories of Prof. *H. Kuhn* (*Max Planck Institute*, Göttingen) and we wish to thank him and Dr. *D. Möbius* for all their help and advice. Some of the first laser experiments on thin films were done in the laboratories of Prof. *F. Schäfer* (*Max Planck Institute*, Göttingen) and we appreciate this help and thank him for his encouragement of our work.

Appendix. – We will derive the eigenvalue equation from the field conditions and the complex reflectivity to give us an expression for the sensitivity enhancement. From two of *Maxwell*'s equations in the rationalized mks system [25] [26] [33]:

$$\nabla \times E = -\frac{\partial \mathrm{B}}{\partial \mathrm{t}} \tag{A1}$$

$$\nabla \times H = \frac{\partial \mathrm{D}}{\partial \mathrm{t}} \tag{A2}$$

we derive with a time periodic traveling wave in the forward z direction

$$E = E_0 \mathrm{e}^{\mathrm{i}(\omega \mathrm{t} - \mathrm{k_z} z)} \tag{A3}$$

and

$$H = H_0 \mathrm{e}^{\mathrm{i}(\omega \mathrm{t} - \mathrm{k_z} z)}, \tag{A4}$$

these equations

$$\nabla \times E = -\mathrm{i}\mu\omega H \tag{A5}$$

$$\nabla \times H = \mathrm{i}\omega\varepsilon E, \tag{A6}$$

where $\omega = 2\pi\nu$; ε is the dielectric function, *i.e.* permittivity which can be complex, μ is the magnetic permeability and $i = \sqrt{-1}$.

For TE propagation we have only to consider the E_y, H_x and H_z components and all partial derivatives with respect to y are assumed to be zero. From A5

$$(\nabla \times E)_x = -\frac{\partial E_y}{\partial z} = ik_z E_y = -i\mu\omega H_x \tag{A7}$$

$$(\nabla \times E)_z = \frac{\partial E_y}{\partial x} = -i\mu\omega H_z \tag{A8}$$

From A6

$$(\nabla \times H)_y = \frac{\partial H_x}{\partial z} - \frac{\partial H_z}{\partial x} = -ik_z H_x - \frac{\partial H_z}{\partial x} = i\omega\varepsilon_y E_y \tag{A9}$$

Substituting A7 and A8 into A9, we obtain the wave equation

$$\frac{\partial^2 E_y}{\partial x^2} + (\varepsilon_y k_0^2 - k_z^2) E_y = 0$$

$$k_x = \sqrt{|\varepsilon_y k_0^2 - k_z^2|}$$

where $k_0 = \omega/c = \omega\sqrt{\varepsilon_0\mu_0}$, the free wave propagation in vacuum. For a three layer system of air, film and substrate shown in *Figure 10* the optical electric field can be written, the propagation in the z direction and time being suppressed (see equ. A3).

$$E_{1y} = A_1 e^{-k_{1x}(x-t)} \qquad t \leq x \tag{A10}$$

$$E_{2y} = A_2 \cos(k_{2x}x + \phi) \qquad 0 \leq x \leq t \tag{A11}$$

$$E_{3y} = A_3 e^{k_{3x}x} \qquad x \leq 0 \tag{A12}$$

where t is the film thickness. Matching both electric (E_y) and magnetic fields ($H_z \propto \partial E_y/\partial_x$ from equ. A8) at each interface we obtain at $x = 0$

$$A_3 = A_2 \cos\phi \tag{A13}$$

and

$$k_{3x}A_3 = k_{2x}A_2 \sin\phi\,. \tag{A14}$$

Then

$$\phi = -\tan^{-1}(k_{3x}/k_{2x} = \beta_{23}) \tag{A15}$$

and

$$A_2 = A_3\sqrt{1+\beta_{23}^2}\,. \tag{A16}$$

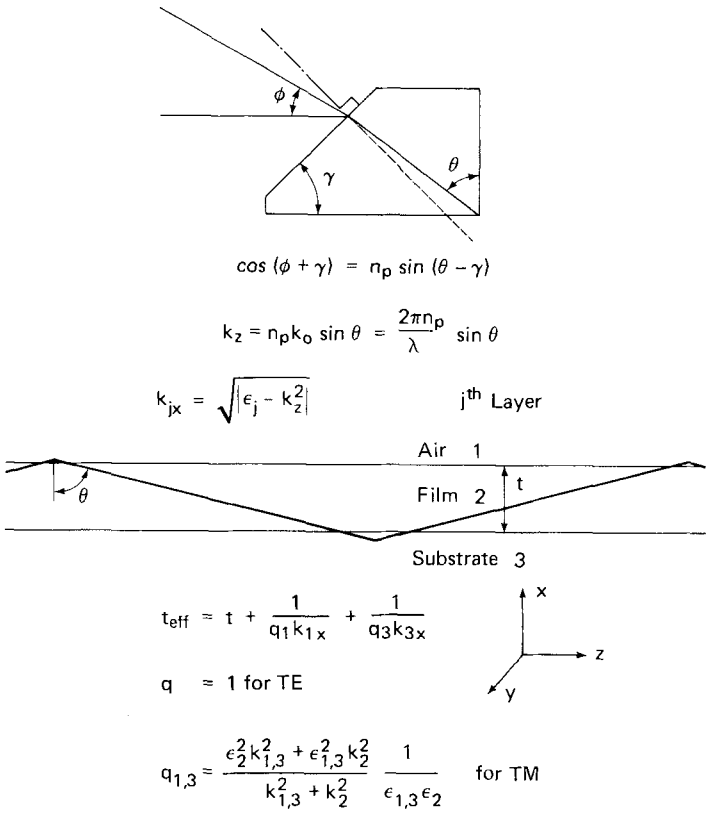

Fig. 10. *Ray optics in a prism, showing the angular relations and the various propagation constants, and ray optics in a wave guide.* Usually θ is from 80° to 90° depending on mode number and refractive index differences (the angle θ here is drawn for convenience closer to 70°). Notice the evanescent wave extension leading to the Goos Hänchen displacement [26].

And at $x = t$

$$A_1 = A_2 \cos(k_{2x}t + \phi) \tag{A17}$$

and

$$-k_{1x}A_1 = -k_{2x}A_2 \sin(k_{2x}t + \phi)\,. \tag{A18}$$

Then

$$\phi = -k_{2x}t + \tan^{-1}\beta_{21} \tag{A19}$$

and

$$A_2 = A_1\sqrt{1+\beta_{21}^2}\,. \tag{A20}$$

Since the phase factor ϕ must be the same in A 15 and A 19 within a multiple of π, we arrive at the well known eigenvalue equation for the non absorbing case:

$$k_{2x}t = m\pi + \tan^{-1}\beta_{21} + \tan^{-1}\beta_{23}\,. \tag{A21}$$

This equation A21 was derived for the TE case. For TM we follow the same procedure but now we have the components H_y, E_x and E_z. From Equ. 6A

$$(\nabla \times H)_x = -\frac{\partial H_y}{\partial z} = ik_z H_y = i\omega\varepsilon_x E_x \tag{A22}$$

and

$$(\nabla \times H)_z = \frac{\partial H_y}{\partial x} = i\omega\varepsilon_z E_z \tag{A23}$$

and from equ. 5A

$$(\nabla \times E)_y = \frac{\partial E_x}{\partial z} - \frac{\partial E_z}{\partial x} = -ik_z E_x - \frac{\partial E_z}{\partial x} = -i\omega\mu H_y, \tag{A24}$$

we obtain as in the TE case equ. A25 by substituting equ. A22 and A23 into A24.

$$\frac{\partial^2 H_y}{\partial x^2} + \left(\varepsilon_z k_0^2 - \frac{\varepsilon_z}{\varepsilon_x} k_z^2\right) H_y = 0 \tag{A25}$$

$$k_x = \sqrt{\left|\varepsilon_z k_0^2 - \frac{\varepsilon_z}{\varepsilon_x} k_z^2\right|} \tag{A26}$$

Note an effect from anisotropy [5] if it exists. From here the procedure to arrive at the eigenvalue equation A21 is the same except that equ. A10–12 are written in terms of H_y, which is matched at each boundary, as well as from equ. A23 $E_z \propto (1/\varepsilon_z)\partial H_y/\partial x$. The ratio β is also modified

$$\beta_{lm} = \frac{k_{mx}/\varepsilon_{mz}}{k_{lx}/\varepsilon_{lz}}, \tag{A27}$$

For the non absorbing case, our APL computer program solves equ. A21 for each mode. Specifically the external angle ϕ is measured for each mode (see *Figure 4*) and converted into the internal angle θ, shown in *Figure 10*, from which k_z is calculated. Since each mode must yield the same thickness, the refractive index is varied until a best fit is obtained for all modes. In cases of good films the errors as little as 30 to 40 Å which is less than 0.2%, have been calculated [5].

When absorbing molecules are introduced, the eigenvalue equ. A21 becomes complex and the solution is more difficult to obtain. A perturbation approach has been used with some success for small absorption, but we found that the use of ray optics [28] and the *Fresnel* equations [33–35] were more convenient. We shall, therefore, briefly outline our matrix procedure [34]. The complex reflectivity at interface l to m is

$$r_{lm} = \frac{1-\beta_{lm}}{1+\beta_{lm}} \tag{A28}$$

and the transmission is

$$\tau_{lm}=\frac{2q}{1+\beta_{lm}}, \qquad \text{where} \qquad q=1 \text{ for TE} \qquad \text{and} \qquad q=\sqrt{\frac{\varepsilon_{lz}}{\varepsilon_{mz}}} \text{ for TM}.$$

As before for TE (s polarization)

$$\beta_{lm}=\frac{k_{mx}}{k_{lx}} \tag{A30}$$

and for TM (p polarization)

$$\beta_{lm}=\frac{k_{mx}/\varepsilon_{mz}}{k_{lx}/\varepsilon_{lz}} \tag{A31}$$

For a multilayer structure a matrix formulation is particularly convenient for computer calculation. We shall follow *Heaven* [34] but because this book is out of print a little more detail will be given. The incident electric field E_1^+ (the plus sign indicating a positive traveling wave, the reflected field E_1^- and the transmitted field E_n^+ are all related by matrix M

$$\begin{pmatrix} E_1^+ \\ E_1^- \end{pmatrix} = M \begin{pmatrix} E_n^+ \\ E_n^- \end{pmatrix}, \tag{A32}$$

($E_n^-=0$ because there is assumed to be no light source below the last layer) where

$$M=M_1 \times M_2 \times M_3 \cdots M_j \cdots M_n. \tag{A33}$$

$$M_j=\frac{1}{\tau_j}\begin{bmatrix} \delta_j & r_j\delta_j \\ r_j d_j^* & \delta_j^* \end{bmatrix} \tag{A34}$$

where

$$\delta_j=e^{ik_{jx}t} \quad \text{and} \quad r_j=r_{j,j+1}. \tag{A35}$$

From these equ. A32

$$R=\frac{|E_1^-|^2}{|E_1^+|^2}=\frac{|M_{21}|^2}{|M_{11}|^2} \tag{A36}$$

and

$$T=\frac{k_{nx}}{k_{1x}}\frac{\left|\prod_{j=1}^{n}\tau_j\right|^2}{|M_{11}|^2}. \tag{A37}$$

It is interesting to note that *Heavens* writes, "Terse through the forms ... the labour involved in the evaluation is considerable ... It is seen that the matrix elements are complex. For a system of transparent layers, the *Fresnel* coefficients are real and the matrices hermitian. For an absorbing layer, the *Fresnel* coefficients for each boundary layer are complex and the resulting matrices non-hermitian.

The case of systems of absorbing films at non-normal incidence, where the angles involved in the expressions for the *Fresnel* coefficients are also complex, is depressing indeed." In contrast we have found the evaluation of equ. A36 and A37 quite straightforward and efficient by an APL program because this computer language was designed for the handling of matrices and vectors. The matrix M_j (A34) was written as a $2\times2\times2$ matrix with real and imaginary parts on different planes and a routine developed to do the complex matrix multiplication. A recursive function, *i.e.*, a function which calls itself, facilitates the stacking of layer on layer. As an example, in *Figure 11* the changes, *i.e.*, broadening and shifts, that occur with increased absorption are shown.

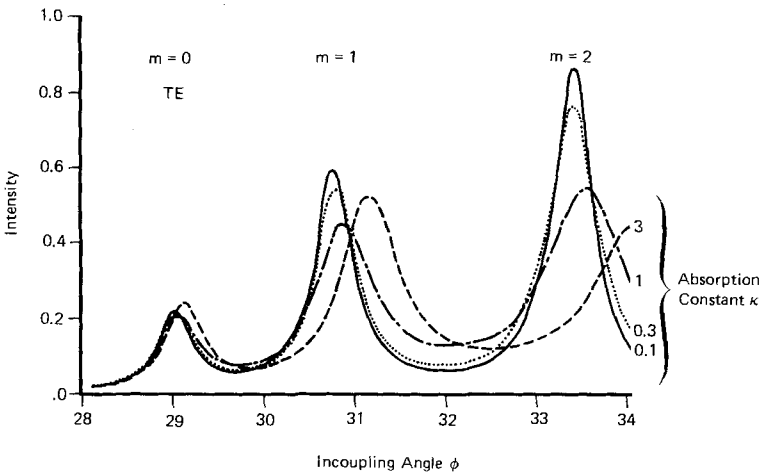

Fig. 11. *Changes in mode patterns with absorption from a monolayer of dye, weakly absorbing to strongly absorbing.* In the complex refractive index $\tilde{n}=n+ik$, the k value was varied from 0.1, 0.3, 1 to 3 while n was fixed at 1.5 (variations connected through the *Kramer-Kröning* relation were neglected). The strong absorption value is approximately that which one would expect for a monolayer of dense packing of dye molecules with an extinction coefficient of 10^5.

The sensitivity of a wave guide absorption experiment can now be derived in terms of the developed results. Consider a unit area of molecular coverage, the absorption of light for perpendicular irradiation is well-known [37]. The power absorbed per unit length

$$P_{abs}=Nh\nu B\rho_E, \tag{A38}$$

where B is the *Einstein* coefficient for stimulated absorption, ρ_E is the energy density, and N is the number of molecules. The power flow is

$$P_{flow}=2\rho_E c/n,$$

where n is the refractive index of the medium and c the velocity of light in space. The ratio is, therefore,

$$P_{abs}/P=nNh\nu B/2c \tag{A39}$$

For a light guide we place this molecular coverage in or on a wave guide. The power transmitted is the integral of the *Poynting* vector across the guide

$$P_{flow} = \frac{1}{2} \int_{-\infty}^{\infty} |E \times H| \, dx \tag{A40}$$

From equ. A7 and A22 we can relate H_x to E_y for TE modes and E_x to H_y for TM modes and integrate E^2 or H^2 to obtain the results

$$P_{flow}^{TE} = \frac{k_z A_2^2}{4\mu\omega} t_{eff}^{TE} \tag{A41}$$

and

$$P_{flow}^{TM} = \frac{k_z A_2^2}{4\varepsilon_{2x}\omega} t_{eff}^{TM}, \tag{A42}$$

where

$$\tau_{eff}^{TE} = \tau + k_{1x}^{-1} + k_{3x}^{-1}, \tag{A43}$$

and

$$t_{eff}^{TM} = t + (q_1 k_{1x})^{-1} + (q_3 k_{3x})^{-1} \tag{A44}$$

with

$$q_j = \frac{\varepsilon_2^2 k_{jx}^2 + \varepsilon_j^2 k_{2x}^2}{\varepsilon_j \varepsilon_2 (k_j^2 + k_2^2)}. \tag{A45}$$

The effective optical thickness of the film is illustrated in *Figure 10* schematically. The displacement at the interfaces is called the *Goos Hänchen* displacement [26] and results from the ray optics approach where the evanescent wave penetrates slightly into the surrounding media. For our typical films of 2 microns thickness the effective thickness is about 15% to 30% thicker, depending of mode number.

Now the power absorbed by equ. A38 requires the evaluations of the field density

$$\rho_E = \frac{1}{2} \varepsilon_2 E^2 = \frac{1}{2} \varepsilon_2 A_2^2 \cos^2(k_{2x} x + \phi) \tag{A46}$$

or

$$= \frac{1}{2} \mu H^2 = \frac{1}{2} \mu A_2^2 \cos^2(k_{2x} x + \phi) \tag{A47}$$

Absorption during transmission reduces the intensity per unit length by the factor

$$\frac{1 - e^{-a}}{a}, \tag{A48}$$

where a is the absorption constant, the imaginary part of k_z. This factor (A48) is readily seen to reduce to one in the limit of small a. Therefore, for the wave guide the ratio is

$$\frac{P_{abs}}{P} = \frac{2Nh\nu B\varepsilon\mu\omega \cos^2(k_{2x} x + \phi)}{k_z t_{eff}} \left(\frac{1 - e^{-a}}{a} \right) \tag{A49}$$

and the ratio of equ. A49 to equ. A39 gives the enhanced sensitivity S.

$$S = \frac{4n_2\omega}{ck_z t_{eff}} \cos^2(k_{2x}x + \phi) \left(\frac{1 - e^{-a}}{a}\right). \tag{A50}$$

To arrive at an estimate of the sensitivity factor S, let us assume a is small so that

$$\frac{1 - e^{-a}}{a} \to 1$$

and we know that the effective index in the guide is bounded $n_2 > n_{eff} > n_3$ and usually n_2 is only a few percent higher than n_3. Therefore,

$$\frac{n_2\omega}{ck_z} \sim 1.$$

and S becomes $4\cos^2(k_{2x}x + \phi)/t_{eff}$.

For a typical case with $t_{eff} \sim 2.4 \times 10^{-4}$ cm, $\cos^2(k_2x + \phi)$ varies from 0.01 at the air interface where it decays rapidly to 0.36 at the substrate interface, with values of 1 at the mode peaks positions in the interior of the film. Hence in this representative case (see *Figure 2*) we arrive at enhancement factors of 215 (m = 0), 830 (m = 1) and 1650 (m = 2) at the air-film interface; 1630 (m = 0), 6300 (m = 1), and 12460 (m = 2) at the film substrate interface; and ~16,700 at the antinodes for any mode – a significant improvement!

REFERENCES

[1] *H. Labhart*, Adv. chem. Physics *13*, 179 (1967).
[2] *J.K. Fischer, D.M. von Brüning & H. Labhart*, Appl. Optics *15*, 2812 (1976).
[3] *H. Kuhn, D. Möbius & H. Bücher*, in 'Techniques of Chemistry', Vol. 1, Part 3B, A. Weissberger & B.W. Rossiter, Eds. John Wiley and Sons Inc., New York 1972.
[4] *J. Tacke, J. Fischer, R. Santo & J.D. Swalen*, Bull. Amer. phys. Soc. *21*, 421 (1976).
[5] *J.D. Swalen, M. Tacke, R. Santo & J. Fischer*, Opt. Commun. *18*, 387 (1976).
[6] *J.D. Swalen, R. Santo, M. Tacke & J. Fischer*, IBM Jour. Res. and Develop. *21*, 168 (1977).
[7] *N.J. Harrick*, 'Internal Reflection Spectroscopy', Wiley-Interscience, New York 1967.
[8] See for example, 'Ellipsometry in the Measurement of Surfaces and Thin Films', Symposia Proceedings 1963, Eds. E. Passaglia, R. Stromberg & J. Kruger, NBS Publication 256.
[9] See for example, *F. Abelès*, 'Methods for Determining Optical Parameters of Thin Films', 'Progress in Optics', Ed. E. Wolf, John Wiley and Sons Inc., New York 1963.
[10] Recent *C.B. Harris*, private communication, has proposed experiments on absorbing molecules by ellipsometry.
[11] *H. Raether*, 'Surface Plasma Oscillations and Their Application', 'Physics of Thin Films', Academic Press, New York-London *9*, 145 (1977).
[12] *K. Holst & H. Raether*, Opt. Commun. *2*, 312 (1970).
[13] *I. Pockrand*, submitted to Surface Science.
[14] *J.J. Cowan & E.T. Arakawa*, Z. Physik *235*, 97 (1970).
[15] *F. Abelès*, Surf. Sci. *56*, 237 (1976).

[16] *F. Abelès & T. Lopez-Rios*, in 'Polaritons', Proc. of the First Taormina Research Conf. on the Structure of Matter, Eds. E. Burstein & F. de Martini, Pergamon Press, Oxford 1972, pp. 241–246.
[17] *I. Pockrand, J. D. Swalen, J. G. Gordon II & M. R. Philpott*, submitted to Surf. Sci.
[18] *J. G. Gordon II & J. D. Swalen*, Opt. Commun. (in press).
[19] *E. Burstein*, Bull. Amer. phys. Soc. *22*, 452 (1977).
[20] *A. Hjortsberg, W. P. Chen, E. Burstein & M. Pomerantz*, Bull. Amer. phys. Soc. *22*, 452 (1977).
[21] *A. Otto*, «Festkörperprobleme XIV» (1974), pp. 1–37.
[22] 'Amer. Inst. of Phys. Handbook', McGraw-Hill Book Co., New York 1963, pp. 6–25 and 6–26.
[23] *Ibid.*, p. 6–13.
[24] *J. D. Swalen, J. Fischer, R. Santo & M. Tacke*, 'Integrated Optics OSA/IEEE Topical Meeting', Salt Lake City, Jan. 1976, reported by *R. Ulrich*, Appl. Optics *15*, 1363 (1976). See also Laser Focus (March 1976), p. 16, and Electro-Optical Systems Design (March 1976), p. 5.
[25] *D. Marcuse*, 'Theory of Dielectric Waveguides', Academic Press, New York 1974, p. 1–19.
[26] *H. Kogelnik*, 'Theory of Dielectric Waveguides', 'Integrated Optics', Ed. T. Tamir, Springer-Verlag, New York 1975, Chap. 2; *F. Goos & H. Hänchen*, Ann. Physik *1*, 333 (1947).
[27] *P. K. Tien & R. Ulrich*, J. opt. Soc. Amer. *60*, 1325 (1970).
[28] *R. Ulrich*, J. opt. Soc. Amer. *60*, 1337 (1970).
[29] *F. Zernike*, 'Fabrication and Measurements of Passive Components', 'Integrated Optics'. Op. cit.
[30] *F. Zernike, J. W. Douglas & D. R. Olson*, J. opt. Soc. Am. *61*, 678 (1971).
[31] *H. P. Weber, F. A. Dunn & W. N. Liebolt*, Appl. Optics *12*, 755 (1973).
[32] *H. R. Anderson & J. D. Swalen* (submitted to Jour. of Adhesion).
[33] *S. Ramo, J. R. Whinnery & T. van Duzer*, 'Fields and Waves in Communication Electronics', John Wiley and Sons, New York 1965.
[34] *O. S. Heavens*, 'Optical Properties of Thin Solid Films', Dover Publications, New York 1965.
[35] *M. V. Klein*, 'Optics', John Wiley and Sons, New York 1970.
[36] *M. Born & E. Wolf*, 'Principles of Optics', Pergamon Press, Oxford 1970.
[37] See for example, *G. Herzberg*, 'Spectra' of Diatomic Molecules', D. van Nostrand Co., New York 1950, p. 20.

85. Synthese von 4-[3β,14-Dihydroxy-5β,14β-androstan-17β-yl]-3-pyrrolin-2-on (Hothesimogenin)

Partialsynthetische Versuche in der Reihe der Herzgifte, 11. Mitteilung [1][2])

von **Theodor W. Güntert, Horst H. A. Linde, Mohamed S. Ragab** und **Sigrid Spengel**

Pharmazeutisches Institut der Universität Basel, Totengässlein 3, 4051 Basel

(17.VI.77)

Synthesis of 4-[3β,14-Dihydroxy-5β,14β-androstan-17β-yl]-3-pyrrolin-2-one (hothesimogenin)

Summary

We describe the synthesis of 4-[3β,14-Dihydroxy-5β,14β-androstan-17β-yl]-3-pyrrolin-2-one (24-aza-24-desoxa-digitoxigenin) (**7**), starting from 3-*O*-acetyl-digitoxigenin (**1**).

[1]) 10. Mitt. siehe [1].
[2]) Über die Pharmakologie von 7 wird an anderer Stelle berichtet werden.